FERMILAB-PUB-96/117-T

arXiv:hep-ph/9605429v1 29 May 1996

One-loop QCD Correction for Inclusive Jet Production and Drell-Yan Process in Composite Models

Taekoon Lee

Fermi National Accelerator Laboratory
P.O. Box 500, Batavia, IL 60510

Abstract

We calculate the one-loop QCD correction for inclusive jet cross section and Drell-Yan process in a general low-energy effective Lagrangian for composite quarks and leptons.

1 Introduction

Recently the CDF group at Fermilab reported a significant excess of one-jet inclusive production at high p_T over the standard QCD prediction [1]. The observed inclusive jet cross section is in excellent agreement with theory, but begins to deviate from the QCD prediction around $p_T = 200$ GeV, and its central value becomes as large as twice the theoretical prediction at p_T above 400 GeV. If this discrepancy between theory and experiment survives more stringent tests, and arises not from the uncertainties in the QCD parameters such as the parton distribution functions but from a genuine new physics, one possible new physics explanation would be existence of a quark substructure.

A substructure in quarks gives rise to four-fermion contact interactions at small energies compared to the compositeness scale Λ via constituent exchanges, and this induces a correction of order s/Λ^2 to the QCD prediction of jet production [2]. The correction is negligible at small energies, but becomes significant at high p_T. This behavior agrees qualitatively with the observed inclusive jet cross section. We assume here that only quarks are composite and gauge fields are elementary.

The CDF fit of the data using the tree level amplitudes from the effective Lagrangian by Eichten, Hinchliffe, Lane and Quigg (EHLQ) [3] with $SU(2)_L$ doublet quarks gives the compositeness scale $\Lambda \approx 1.6$ TeV. To go beyond the tree level analysis of the data, we need the QCD one-loop corrected amplitudes for $q_i q_j \to q_i q_j$. The leading QCD correction to the amplitudes arising from the QCD interaction has been known [4, 5, 6], and so only the one-loop correction to the terms arising from the four-fermion contact interactions needs to be computed.

In this paper, we calculate the one-loop QCD correction to $q_i q_j \to q_i q_j$ in the EHLQ effective Lagrangian, using the framework of Kunszt,et.al. for one-jet inclusive cross section [6, 7], and also discuss QCD corrections in Drell-Yan process. Section 2 through 6 is devoted to QCD corrections for the inclusive one-jet cross section. In sec. 2 and 3, we review the EHLQ Lagrangian, and give the squared amplitudes at tree-level, and in sec.4 discuss the ultraviolet divergence and summarize the short distant effects of loop corrections. In sec.5 we briefly review the method by Kunszt,et.al. for one-loop inclusive jet cross section, and give our result in sec.6. Details of QCD calculation may be found in the appendix. Finally in sec. 7 we discuss QCD corrections in Drell-Yan process.

2 Effective action

A typical term of the helicity conserving effective interactions of composite quarks at low energies compared to the compositeness scale can be written in the form of current product

$$\mathcal{L}_{int}(0) = g_0^2 \eta(\mu, \Lambda) \int J_\mu^R(\mu, x) J_\nu^R(\mu, 0) D_{\mu\nu}(x, \Lambda) d^4x, \tag{1}$$

where $\eta(\mu,\Lambda)$ and J_μ^R are renormalized effective coupling and generic quark current respectively. The constituent exchange between currents is represented by $D_{\mu\nu}(x,\Lambda)$ which is assumed to satisfy

$$D_{\mu\nu}(x,\Lambda) = \Lambda^2 g_{\mu\nu} D(x\Lambda), \tag{2}$$

$$D_{\mu\nu}(x,\Lambda) \to g_{\mu\nu}\frac{1}{\Lambda^2}\delta^{(4)}(x) \quad \text{for} \quad x\Lambda \gg 1. \tag{3}$$

The Λ in $D_{\mu\nu}$ is a cutoff that determines the interaction range of the constituent exchanges. The relation between $\eta(\mu,\Lambda)$, J_μ^R and the corresponding bare quantities depends on the fundamental dynamics at the compositeness scale. However, this model dependence does not cause any problem in calculating QCD corrections at low energies because any ambiguity arising from the lack of knowledge on how the currents and couplings are renormalized can be absorbed in the coupling η which is supposed to be determined experimentally. With (3), (1) becomes at tree level

$$\frac{g_0^2\eta}{\Lambda^2}\, J_\mu\, J^\mu. \tag{4}$$

The most general helicity conserving, $SU(3)_c \times SU(2)_L \times U_Y(1)$ symmetric low-energy effective Lagrangian of up and down quarks by EHLQ is

$$\begin{aligned}
\mathcal{L}_{EHLQ} = {} & g^2\left(\frac{g_0^2}{2g^2\Lambda^2}\right)\Big\{\eta_0\bar{q}_L\gamma^\mu\bar{q}_L\bar{q}_L\gamma^\mu q_L + \eta_1\bar{q}_L\gamma^\mu\frac{\tau^a}{2}q_L\bar{q}_L\gamma^\mu\frac{\tau^a}{2}q_L \\
& +\eta_u\bar{q}_L\gamma^\mu q_L\bar{u}_R\gamma^\mu u_R + \eta_d\bar{q}_L\gamma^\mu q_L\bar{d}_R\gamma^\mu d_R \\
& +\eta_{8u}\bar{q}_L\gamma^\mu\frac{\lambda^a}{2}q_L\bar{u}_R\gamma^\mu\frac{\lambda^a}{2}u_R + \eta_{8d}\bar{q}_L\gamma^\mu\frac{\lambda^a}{2}q_L\bar{d}_R\gamma^\mu\frac{\lambda^a}{2}d_R \\
& +\eta_{uu}\bar{u}_R\gamma^\mu u_R\bar{u}_R\gamma^\mu u_R + \eta_{dd}\bar{d}_R\gamma^\mu d_R\bar{d}_R\gamma^\mu d_R \\
& +\eta_{ud}\bar{u}_R\gamma^\mu u_R\bar{d}_R\gamma^\mu d_R + \eta'_{ud}\bar{u}_R\gamma^\mu d_R\bar{d}_R\gamma^\mu u_R\Big\},
\end{aligned} \tag{5}$$

where $q_L = (u_L, d_L)$. We inserted in (5) the strong coupling g^2 explicitly to make the tree amplitudes of QCD and contact terms be formally in the same order in the QCD coupling. For convenience, in the rest of the paper we absorb the factor

$$\frac{g_0^2}{2g^2\Lambda^2} \tag{6}$$

into the coupling η's. We also assume here all quarks are massless . Then because of the $SU_L(2)$ symmetry, there are only seven independent helicity amplitudes for $q_iq_j \to q_iq_j$. They are: $u_Ld_L \to u_Ld_L, u_Lu_L \to u_Lu_L, u_Rd_L \to u_Rd_L, u_Ld_R \to u_Ld_R, u_Ru_R \to u_Ru_R, d_Rd_R \to d_Rd_R$, and $u_Rd_R \to u_Rd_R$. The amplitude for $d_Ld_R \to d_Ld_R$, for example, is identical to that of $u_Ld_R \to u_Ld_R$ because of the $SU(2)_L$ symmetry. In the following, we calculate these seven amplitudes to one-loop order in QCD.

3 Tree amplitudes

The tree level amplitudes for the helicity channels in the EHLQ effective action are given in the appendix. Note that we follow the notation in ref. [7, 8] for the helicity amplitude and spinor algebra.

The squared amplitudes— color and spin averaged —for quark channels are

$$\begin{aligned}|\mathcal{A}(ud\to ud)|^2 &= \left|\mathcal{A}(\bar{u}\bar{d}\to\bar{u}\bar{d})\right|^2 = \\ &g^4\left[\frac{4}{9}\frac{s^2+u^2}{t^2}+u^2\left(\eta_u^2+\eta_d^2+\frac{2}{9}(\eta_{8u}^2+\eta_{8d}^2)\right)\right. \\ &+s^2(4\eta_0^2+\frac{2}{3}\eta_0\eta_1+\frac{11}{12}\eta_1^2+\frac{2}{3}\eta_{ud}\eta'_{ud}+\eta_{ud}^2+\eta_{ud}'^2) \\ &\left.+\frac{8}{9}\frac{s^2}{t}(\eta_1+\eta'_{ud})+\frac{4}{9}\frac{u^2}{t}(\eta_{8u}+\eta_{8d})\right], \end{aligned} \tag{7}$$

$$\begin{aligned}|\mathcal{A}(uu\to uu)|^2 &= |\mathcal{A}(\bar{u}\bar{u}\to\bar{u}\bar{u})|^2 = \\ &g^4\left[\frac{4}{9}\left(\frac{s^2+u^2}{t^2}+\frac{s^2+t^2}{u^2}-\frac{2s^2}{3tu}\right)\right. \\ &+\frac{4}{9}\left(\frac{s^2}{t}+\frac{s^2}{u}\right)(4\eta_0+\eta_1+4\eta_{uu})+\frac{8}{9}\eta_{8u}\left(\frac{u^2}{t}+\frac{t^2}{u}\right) \\ &\left.+\frac{2s^2}{3}(16\eta_0^2+8\eta_0\eta_1+\eta_1^2+16\eta_{uu}^2)+2(u^2+t^2)(\eta_u^2+\frac{2}{9}\eta_{8u}^2)\right], \end{aligned} \tag{8}$$

and using the crossing symmetry

$$\left|\mathcal{A}(u\bar{d}\to u\bar{d})\right|^2 = |\mathcal{A}(\bar{u}d\to\bar{u}d)|^2 = |\mathcal{A}(ud\to ud)|^2\,(s\leftrightarrow u), \tag{9}$$

$$\left|\mathcal{A}(\bar{u}\bar{u}\to\bar{d}\bar{d})\right|^2 = \left|\mathcal{A}(d\bar{d}\to\bar{u}\bar{u})\right|^2 = |\mathcal{A}(ud\to ud)|^2\,(s\to u, t\to s, u\to t), \tag{10}$$

$$|\mathcal{A}(u\bar{u}\to u\bar{u})|^2 = |\mathcal{A}(uu\to uu)|^2\,(s\leftrightarrow u), \tag{11}$$

with

$$s=(p_1+p_2)^2,\ t=(p_1-p_4)^2,\ u=(p_1-p_3)^2. \tag{12}$$

For the channels involving d-quarks only, we can obtain the squared amplitudes by replacing η_{uu}, η_{8u} with η_{dd}, η_{8d} respectively in (8),(11).

Putting back the factor

$$\frac{g_0^2/4\pi}{2\alpha_s\Lambda^2} \tag{13}$$

into each η's in the above equations and keeping only η_0 we can recover the formulas in [3] with

$$g_0^2/4\pi = 1. \tag{14}$$

Note that we have corrections for typos in (8.13), (8.15) in [3].

4 Ultraviolet divergence

The one-loop Feynman diagrams for $q_i q_j \to q_i q_j$ in the EHLQ effective Lagrangian are given in Fig.1. In the massless limit, the one-loop self energy diagrams for fermions in the dimensional regularization vanish [10], and (g),(h) in Fig.1 are the UV counter terms for current renormalization arising from the fermion self-energy diagrams and (a),(b). (g),(h) are required only for color octet currents, and the counter terms for the conserved, color singlet currents vanish. We do not include in our calculation the one-loop diagram in Fig.2(b) because its finite part coming from the small momentum region ($\sim \sqrt{s}$) is suppressed by a factor s/Λ^2 relative to those in Fig.1. This can be easily seen from the fact that the four-fermion-gluon vertex in the diagram is given by the effective Lagrangian

$$\sim \frac{1}{\Lambda^4} f_{abc}\, J^a_\mu\, J^b_\nu F^c_{\mu\nu} \tag{15}$$

represented in Fig.2(a). Here J^a_μ denote color octet currents. The contribution from the large momentum region ($\gg \sqrt{s}$), which is dependent on the fundamental dynamics at the compositeness scale, is independent of external momenta, and renormalizes only the couplings of the contact terms. Since we are not interested in how the η's are renormalized, we can completely exclude this diagram.

There are also penguin diagrams (Fig.3). Although they are not one-loop QCD corrections, it is easy to see that they induce form factors in the quark-gluon vertices that are formally of same order of magnitude as the QCD one-loop corrections. The form factors induced by the penguin diagrams assume the form

$$\begin{aligned} F(q^2) &= 1 + \frac{\eta g_0^2}{(4\pi)^2} C(\ln(-q^2)) \left(\frac{q^2}{\Lambda^2}\right) \\ &\approx 1 + \bar{C} \frac{\eta g_0^2}{(4\pi)^2} \left(\frac{q^2}{\Lambda^2}\right), \end{aligned} \tag{16}$$

where $C\left(\ln(-q^2)\right)$ is a model dependent function of $O(1)$. In the last step we replaced the function C with its average value $\bar{C}$ in the momentum range of interest. Thus penguin diagrams introduce new free parameters in the amplitudes. This form factor effect from penguin diagrams may be combined with that in the vector boson propagators [9, 3].

Now in general, (a)-(f) have ultraviolet divergences as well as soft and collinear divergences. For one-jet inclusive cross section, the soft and collinear divergences are cancelled by those from $2 \to 3$ process, which will be reviewed in more detail in the next section. The UV divergences in (a), (b), as mentioned before, are cancelled by the counter terms (g),(h). We assume the counter terms are given in the $\overline{MS}$ scheme. The scheme dependence of the counter terms is absorbed in the coupling η's to render the physical amplitudes scheme independent. The UV divergences in (c)-(f) arise from the approximation in (3). If we insert $D_{\mu\nu}(x, \Lambda)$ between the currents, the diagrams would be finite with logarithmic terms of order $\alpha_s \log(\Lambda)$ from the

short distance region. The scale Λ plays the role of an UV cutoff. The logarithmic terms can be summed to all orders in QCD in the leading log approximation by applying RG-improved operator product expansion to (1) [11, 12, 13]. Applying OPE to $J^R_\mu(x)J^R_\nu(0)$,

$$\int J^R_\mu(x)J^R_\nu(0)D_{\mu\nu}(x,\Lambda)dx = \sum_i c_i(\mu/\Lambda,\alpha(\mu))O^R_i(0), \tag{17}$$

with c_i satisfying

$$\left(\mu^2\frac{\partial}{\mu^2} + \beta(\alpha)\frac{\partial}{\partial\alpha} + \tilde{\gamma}_i(\alpha)\right)c_i(\mu/\Lambda,\alpha(\mu)) = 0, \tag{18}$$

where

$$\tilde{\gamma}_i = 2\gamma_J - \gamma_i, \tag{19}$$

and γ_J, γ_i are the anomalous dimensions of the current and the operator O_i respectively, and

$$\begin{aligned}\beta(\alpha) &= \mu^2\frac{\partial}{\partial\mu^2}\alpha = -\beta_0\alpha^2(1+O(\alpha)),\\ \beta_0 &= \frac{1}{4\pi}(11-\frac{2}{3}N_f),\end{aligned} \tag{20}$$

$$\tilde{\gamma}_i(\alpha) = \tilde{\gamma}_i{}^{(1)}\alpha + O(\alpha^2). \tag{21}$$

Note that $\tilde{\gamma}_i$ arises only from the UV divergences in diagram (c)-(f).

Integrating the RG equation,

$$\begin{aligned}c_i(\mu/\Lambda,\alpha(\mu)) &= c_i(\alpha(\Lambda))\exp\left(\int_{\alpha(\mu)}^{\alpha(\Lambda)}\frac{\tilde{\gamma}_i(\alpha)}{\beta(\alpha)}d\alpha\right),\\ &\approx c_i^{(0)}L_i(\alpha(\mu),\alpha(\Lambda))\end{aligned} \tag{22}$$

where

$$L_i(\alpha(\mu),\alpha(\Lambda)) = \left(\frac{\alpha(\mu)}{\alpha(\Lambda)}\right)^{\frac{\tilde{\gamma}_i^{(1)}}{\beta_0}}. \tag{23}$$

The constants $c_i^{(0)}$ can be determined from the tree-level amplitudes. Substituting (22) into (17), the one-loop effective Lagrangian for (1) should read

$$\mathcal{L}_{int}(0) = \sum g_0^2\eta(\mu,\Lambda)c_i^0L_iO_i^R. \tag{24}$$

In computing the matrix element $<f|O_i^R|i>$, we take the $\overline{MS}$ subtraction scheme for the UV divergences. The scheme dependence in the matrix element is compensated by that of c_i to make physical amplitudes scheme independent.

Since the EHLQ effective action at one-loop must assume the same form as in the tree-level action, the short distance effect in diagram (c)-(f) results in as a mixing among η's with an

appropriate scaling by L_i. Let us first consider $u_L d_L \to u_L d_L$ process. The effective Lagrangian for this process is

$$\begin{aligned}\mathcal{L}_{u_L d_L} &= (2\eta_0 - \frac{\eta_1}{2})O_1 + \eta_1 O_2 \\ &= (2\eta_0 + \frac{\eta_1}{2})O_+ + (\frac{3\eta_1}{2} - 2\eta_0)O_-, \end{aligned} \tag{25}$$

where

$$\begin{aligned}O_1 &= \bar{u}_L\gamma^\mu u_L \bar{d}_L\gamma^\mu d_L, \\ O_2 &= \bar{u}_L\gamma^\mu d_L \bar{d}_L\gamma^\mu u_L, \end{aligned} \tag{26}$$

and

$$O_\pm = \frac{1}{2}(O_2 \pm O_1). \tag{27}$$

Because $O_+(O_-)$ is symmetric (anti-symmetric) under interchange between up and down quarks and separately up and down anti-quarks, $O_\pm$ are multiplicatively renormalized to all orders in QCD, and their anomalous dimensions at one-loop are given by [13]

$$\gamma_\pm^{(1)} = \mp\frac{3}{4\pi N_c}(N_c \mp 1). \tag{28}$$

According to (24), the effective action at one-loop is

$$\begin{aligned}\mathcal{L}_{u_L d_L} \to \quad & (2\eta_0 + \frac{\eta_1}{2})L_+ O_+^R + (\frac{3\eta_1}{2} - 2\eta_0)L_- O_-^R \\ = \; & \frac{1}{2}\left((2\eta_0 + \frac{\eta_1}{2})L_+ - (\frac{3\eta_1}{2} - 2\eta_0)L_-\right) O_1^R \\ + \; & \frac{1}{2}\left((2\eta_0 + \frac{\eta_1}{2})L_+ + (\frac{3\eta_1}{2} - 2\eta_0)L_-\right) O_2^R, \end{aligned} \tag{29}$$

with

$$L_\pm(\alpha(\mu), \alpha(\Lambda)) = \left(\frac{\alpha(\mu)}{\alpha(\Lambda)}\right)^{-\frac{\gamma_\pm^{(1)}}{\beta_0}}. \tag{30}$$

Thus at one-loop order we have to replace η_0, η_1 by $\bar{\eta}_0, \bar{\eta}_1$ defined by

$$\begin{pmatrix} \bar{\eta}_0 \\ \bar{\eta}_1 \end{pmatrix} = \begin{pmatrix} \frac{3}{4}L_+ + \frac{1}{4}L_- & \frac{3}{16}(L_+ - L_-) \\ L_+ - L_- & \frac{1}{4}L_+ + \frac{3}{4}L_- \end{pmatrix} \begin{pmatrix} \eta_0 \\ \eta_1 \end{pmatrix}. \tag{31}$$

Let us now consider $u_L d_R \to u_L d_R$ which involves a color octet current. The Lagrangian for this process is

$$\mathcal{L}_{u_L d_R} = \eta_d O_1 + \eta_{8d} O_2 \tag{32}$$

where O_i now are defined by

$$\begin{aligned} O_1 &= \bar{u}_L\gamma^\mu u_L \bar{d}_R\gamma^\mu d_R \\ O_2 &= \bar{u}_L\gamma^\mu \frac{\lambda^a}{2} u_L \bar{d}_L\gamma^\mu \frac{\lambda^a}{2} d_R. \end{aligned} \tag{33}$$

Unlike in the previous example, in this case there is no simple symmetry argument to find multiplicatively renormalized operators, and so we are going to diagonalize the one-loop mixing matrix explicitly.

From the UV divergence part in (a)-(f), we have

$$\begin{pmatrix} O_1 \\ O_2 \end{pmatrix}^B = Z \begin{pmatrix} O_1 \\ O_2 \end{pmatrix}^R, \tag{34}$$

where

$$Z = \begin{pmatrix} 1 & \frac{6g^2}{(4\pi)^2}\frac{1}{\epsilon} \\ \frac{3(N_c^2-1)g^2}{2N_c^2(4\pi)^2}\frac{1}{\epsilon} & 1+\frac{3(N_c^2-2)g^2}{N_c(4\pi)^2}\frac{1}{\epsilon} \end{pmatrix} \tag{35}$$

with $\epsilon = \frac{1}{2}(4-n)$. The one-loop anomalous dimension of O_i is then

$$\Gamma = \frac{\alpha_s}{4\pi}\begin{pmatrix} 0 & 6 \\ \frac{4}{3} & 7 \end{pmatrix}. \tag{36}$$

Diagonalizing Γ, we have

$$L\Gamma L^{-1} = \frac{\alpha_s}{4\pi}\begin{pmatrix} -1 & 0 \\ 0 & 8 \end{pmatrix} \tag{37}$$

with

$$L = \begin{pmatrix} 1 & -\frac{3}{4} \\ \frac{4}{27} & \frac{8}{9} \end{pmatrix}. \tag{38}$$

The one-loop anomalous dimension of octet current arising from (a) in Fig.1 is

$$\gamma_{j_8}^{(1)} = -\frac{N_c}{8\pi}. \tag{39}$$

Thus at one-loop level,

$$\mathcal{L}_{u_L d_R} \to \bar{\eta}_d O_1^R + \bar{\eta}_{8d} O_2^R \tag{40}$$

where

$$\begin{pmatrix} \bar{\eta}_d \\ \bar{\eta}_{8d} \end{pmatrix} = \begin{pmatrix} c_1 & d_1 \\ c_2 & d_2 \end{pmatrix}\begin{pmatrix} \eta_d \\ \eta_{8d} \end{pmatrix}, \tag{41}$$

$$\begin{pmatrix} c_1 \\ c_2 \end{pmatrix} = L^t \begin{pmatrix} L_{8+} & 0 \\ 0 & L_{8-} \end{pmatrix}\left(L^{-1}\right)^t \begin{pmatrix} 1 \\ 0 \end{pmatrix}, \tag{42}$$

$$\begin{pmatrix} d_1 \\ d_2 \end{pmatrix} = L^t \begin{pmatrix} \tilde{L}_{8+} & 0 \\ 0 & \tilde{L}_{8-} \end{pmatrix} \left(L^{-1}\right)^t \begin{pmatrix} 0 \\ 1 \end{pmatrix}, \tag{43}$$

and

$$\begin{aligned} L_{8\pm} &= \left(\frac{\alpha(\mu)}{\alpha(\Lambda)}\right)^{-\gamma^{(1)}_{8\pm}/\beta_0}, \\ \tilde{L}_{8\pm} &= \left(\frac{\alpha(\mu)}{\alpha(\Lambda)}\right)^{-(\gamma^{(1)}_{8\pm}-2\gamma^{(1)}_{j_8})/\beta_0}, \end{aligned} \tag{44}$$

with

$$\begin{aligned} \gamma^{(1)}_{8+} &= \frac{-1}{4\pi} \\ \gamma^{(1)}_{8-} &= \frac{8}{4\pi}. \end{aligned} \tag{45}$$

Similar calculation gives

$$\begin{pmatrix} \bar{\eta}_{uu} \\ \bar{\eta}_{dd} \end{pmatrix} = \begin{pmatrix} L_+ & 0 \\ 0 & L_- \end{pmatrix} \begin{pmatrix} \eta_{uu} \\ \eta_{dd} \end{pmatrix}, \tag{46}$$

and

$$\begin{pmatrix} \bar{\eta}_{ud} \\ \bar{\eta}'_{ud} \end{pmatrix} = \frac{1}{2} \begin{pmatrix} L_+ + L_- & L_+ - L_- \\ L_+ - L_- & L_+ + L_- \end{pmatrix} \begin{pmatrix} \eta_{ud} \\ \eta'_{ud} \end{pmatrix}, \tag{47}$$

where $L_\pm$ are defined in (30). The transformation for η_u, η_{8u} can be obtained by replacing η_d, η_{8d} in (41) with η_u, η_{8u} respectively. The modified coupling $\bar{\eta}$'s should also be used in calculating the $2 \to 3$ tree-level amplitudes. For notational convenience, we keep using η's instead of the modified couplings; however, in the rest of the paper, all η's should be understood as $\bar{\eta}$'s defined in (31), (41), (46), and (47).

5 Calculation framework

When computing the one-jet inclusive cross section, we need the one-loop QCD amplitudes for $2 \to 2$, not the squared amplitudes, since QCD and the composite model interaction act coherently. To use the one-loop QCD helicity amplitudes for $2 \to 2$ by Kunszt,et.al. [6] calculated in the 't Hooft Veltman scheme [14], we also calculate the diagrams in Fig.1 in the 't Hooft Veltman scheme. Kunszt,et.al. also isolated the soft and collinear divergences in $2 \to 2$ and $2 \to 3$ processes, exposed explicitly the cancellation of these divergences among them,

and gave a complete prescription for the one-jet inclusive cross section [6, 7]. In this section we briefly review the calculation scheme of Kunszt,et.al., and identify terms to be calculated for the one-jet cross section. We follow the notation in [6, 7] and readers should consult the references for more detailed discussions.

The one-jet inclusive cross section

$$I = \frac{d\sigma_{jet}}{dp_J dy_J} \tag{48}$$

can be written as

$$I = I(2 \to 2) + I(2 \to 3), \tag{49}$$

where

$$\begin{aligned} I(2 \to 2) &= \frac{1}{2!} \int d\rho_2 \frac{d\sigma(2 \to 2)}{d\rho_2} S_2(p_1^\mu, p_2^\mu) \\ I(2 \to 3) &= \frac{1}{3!} \int d\rho_3 \frac{d\sigma(2 \to 3)}{d\rho_3} S_3(p_1^\mu, p_2^\mu, p_3^\mu) \end{aligned} \tag{50}$$

and

$$\begin{aligned} d\rho_2 &= dy_1 dp_2 dy_2 d\phi_2 \\ d\rho_3 &= dy_1 dp_2 dy_2 d\phi_2 dp_3 dy_3 d\phi_3. \end{aligned} \tag{51}$$

S_2, S_3 define a jet algorithm, and p_i, y_i denote transverse momenta and pseudo-rapidities of the partons respectively.

$I(2 \to 2)$ can be divided into singular ($\sim 1/\epsilon^p$) and nonsingular parts

$$I(2 \to 2) = I(2 \to 2)_S + I(2 \to 2)_{NS} \tag{52}$$

with

$$I(2 \to 2)_{NS} = \frac{\alpha_s^2}{2s^2} \int d\rho_2 p_2 \sum_{\mathbf{a}} L_{AB} \left(\psi^{(4)}(\mathbf{a}, \mathbf{p}) + \frac{\alpha_s}{2\pi} \psi^{(6)}_{NS}(\mathbf{a}, \mathbf{p}) \right) S_2(p_1^\mu, p_2^\mu), \tag{53}$$

where

$$L_{AB} = \frac{f_A(a_A, x_A) f_B(a_B, x_B)}{w(a_A) x_A w(a_B) x_B}, \tag{54}$$

and $\mathbf{a} = (a_A, a_B, a_1, a_2)$ for parton flavors, and $\mathbf{p} = (p_A, p_B, p_1, p_2)$. Indices A, B and $1, 2$ denote the initial state and the final state partons respectively. $\psi^{(4)}$ is the Born amplitude squared and $\psi^{(6)}_{NS}$ is the nonsingular part of $\psi^{(6)}$ defined in

$$\sum_{\substack{colors \\ spins}} |\mathcal{A}(a_A + a_B \to a_1 + a_2)|^2 = g^4 \left(\psi^{(4)}(\mathbf{a}, \mathbf{p}) + 2g^2 c_\Gamma \left(\frac{\mu^2}{Q^2_{ES}} \right)^\epsilon \psi^{(6)}(\mathbf{a}, \mathbf{p}) + O(g^4) \right) \tag{55}$$

where Q_{ES} is an arbitrary scale introduced by Ellis and Sexton [4], and

$$c_\Gamma = \frac{1}{(4\pi)^{2-\epsilon}} \frac{\Gamma(1-\epsilon)^2\Gamma(1+\epsilon)}{\Gamma(1-2\epsilon)}. \tag{56}$$

The singular part $I(2\to 2)_S$ depends only on the Altarelli-Parisi functions and the tree-level amplitudes in four dimensions, $\psi^{(4)}(\mathbf{a},\mathbf{p})$ and $\psi^{(4,c)}_{mn}(\mathbf{a},\mathbf{p})$, with the latter defined by

$$\psi^{(4,c)}_{mn}(\mathbf{a},\mathbf{p}) = \frac{-2}{g^4} T^a_{c_{\bar m}c_m} T^a_{c_{\bar n}c_n} \prod_{i\neq m,n} \delta_{c_{\bar i}c_i} \mathcal{A}^{(0)}_{c_A c_B c_1 c_2}(2\to 2) \mathcal{A}^{(0)*}_{c_{\bar A}c_{\bar B}c_{\bar 1}c_{\bar 2}}(2\to 2). \tag{57}$$

For $\mathbf{a} = (q_i, q_j, q_i, q_j)$, $T^a = \lambda^a/2$ for the final state quarks and $T^a = -\left(\lambda^a\right)^t/2$ for the initial state quarks.

Similarly $I(2\to 3)$ can be divided into singular and nonsingular parts

$$\begin{aligned} I(2\to 3) &= \left[I(2\to 3) - \sum_n I'_n(2\to 3)\right] + \sum_n I'_n(2\to 3) \\ &= I_{finite}(2\to 3) + \sum_n I'_n(2\to 3) \end{aligned} \tag{58}$$

where n runs over $A, B, 1, 2$. The soft and collinear divergences are contained in $I'_n(2\to 3)$, and $I'_n(2\to 3)$ is divergent only when p_3 becomes soft or collinear to the parton n. $I_{finite}(2\to 3)$ is by construction well defined over all parton phase space, depends only on the tree-level amplitudes in four dimensions, and so the phase-space integration can be done numerically.

Separating collinear divergence from soft divergence, $I'_n(2\to 3)$ can be written as

$$I'_n(2\to 3) = I^{soft}_n(2\to 3) + I^{coll}_n(2\to 3), \tag{59}$$

with

$$\begin{aligned} I^{soft}_n(2\to 3) &= I^{soft}_n(2\to 3)_S + I^{soft}_n(2\to 3)_{NS} \\ I^{coll}_n(2\to 3) &= I^{coll}_n(2\to 3)_S + I^{coll}_n(2\to 3)_{NS}, \end{aligned} \tag{60}$$

where the explicit form of each term is given in [6, 7]. The singular and nonsingular terms in (60) involve Altarelli-Parisi functions and only tree-level amplitudes in four dimensions. For example,

$$I^{soft}_2(2\to 3)_{NS} = \frac{\alpha_s^3}{4\pi s^2} \int d\rho_2 p_2 \sum_{\mathbf{a}} L_{AB} \left[\psi^{soft}_2(\mathbf{a},\mathbf{p})\right]_{NS} S_2(p_1^\mu, p_2^\mu) \tag{61}$$

with

$$\left[\psi^{soft}_2\right]_{NS} = \sum_{m=A,B,1} \psi^{(4,c)}_{2m}\ \tilde T_{2m}, \tag{62}$$

where $\tilde T_{2m}$ is a universal function of $s_{ij} = (p_i + p_j)^2$.

Adding (58) into (52), we have

$$I = I(2 \to 2)_{NS} + \sum_n \left(I_n^{soft}(2 \to 3)_{NS} + I_n^{coll}(2 \to 3)_{NS} \right) + I_{finite}(2 \to 3) \tag{63}$$

with complete cancellation of the singular terms. From (63) we see that for the one-jet inclusive cross section, we need to calculate the tree-level amplitude $\psi^{(4)}, \psi_{mn}^{(4,c)}$ in four dimensions, and the one-loop amplitudes $\psi_{NS}^{(6)}$ of $\psi^{(6)}$ defined in (55).

6 One-loop amplitudes

The general form of the amplitude for $q_i(p_1)q_j(p_2) \to q_k(p_3)q_l(p_4)$ to one-loop for each helicity channel can be written as

$$\mathcal{A}(p_1 + p_2 \to p_3 + p_4) = g^2 \tilde{c}\, (A\, \delta_{li}\delta_{kj} + B\, \delta_{lj}\delta_{ki}), \tag{64}$$

where

$$\begin{aligned} A &= A^{(0)} + g^2 A^{(1)} \\ B &= B^{(0)} + g^2 B^{(1)}, \end{aligned} \tag{65}$$

and

$$A^{(i)} = A_{QCD}^{(i)} + A_{cont}^{(i)}, \quad B^{(i)} = B_{QCD}^{(i)} + B_{cont}^{(i)}. \tag{66}$$

$\tilde{A}_{QCD}^{(i)}, \tilde{B}_{QCD}^{(i)}$ and $\tilde{A}_{cont}^{(i)}, \tilde{B}_{con}^{(i)}$ are the tree and one-loop amplitudes arising from QCD and the fermion contact interactions respectively, and $\tilde{c}$ is a channel dependent spinor matrix element.

The amplitude squared for each helicity channel is then

$$\begin{aligned} \sum_{colors} |\mathcal{A}|^2 &= g^4 |\tilde{c}|^2 N_c^2 \left\{ \left(A^{(0)}\right)^2 + \left(B^{(0)}\right)^2 + \frac{2}{N_c} A^{(0)} B^{(0)} + 2g^2 \left[A^{(0)} Re(A^{(1)}) \right.\right. \\ &\quad \left.\left. + B^{(0)} Re(B^{(1)}) + \frac{1}{N_c} \left(A^{(0)} Re(B^{(1)}) + B^{(0)} Re(A^{(1)}) \right) \right] \right\}. \end{aligned} \tag{67}$$

Comparing (67) with (55), we have $\psi^{(4)}, \psi_{NS}^{(6)}$ in $q_i q_j \to q_i q_j$ channel,

$$\begin{aligned} \psi^{(4)} &= \sum_{spins} |\tilde{c}|^2 N_c^2 \left[\left(A^{(0)}\right)^2 + \left(B^{(0)}\right)^2 + \frac{2}{N_c} A^{(0)} B^{(0)} \right] \\ \psi_{NS}^{(6)} &= \sum_{spins} |\tilde{c}|^2 N_c^2 \left[A^{(0)} Re(\tilde{A}^{(1)}) + B^{(0)} Re(\tilde{B}^{(1)}) + \frac{1}{N_c} (A^{(0)} Re(\tilde{B}^{(1)}) + B^{(0)} Re(\tilde{A}^{(1)})) \right], \end{aligned} \tag{68}$$

where

$$\begin{aligned}\tilde{A}^{(1)} &= \left[\left(\frac{Q_{ES}^2}{\mu^2}\right)^{\epsilon}\frac{1}{c_\Gamma}A^{(1)}\right]_{NS}\\ \tilde{B}^{(1)} &= \left[\left(\frac{Q_{ES}^2}{\mu^2}\right)^{\epsilon}\frac{1}{c_\Gamma}B^{(1)}\right]_{NS}.\end{aligned} \tag{69}$$

For the one-loop amplitudes $A^{(1)}_{cont}, B^{(1)}_{cont}$, we calculate the diagrams in Fig.1 in the 't Hooft Veltman dimensional regularization scheme in which the spins and momenta of internal particles are defined in n dimensions, while those of external particles are defined in four dimensions. The calculation of the one-loop diagrams in the 't Hooft Veltman scheme is much simplified since we can treat the Dirac γ matrices as if they were defined in four dimensions. To show this, let us consider, as an example, the diagram (a) in Fig.1 for $u_L(p_1)d_L(p_2) \to u_L(p_4)d_L(p_3)$. The diagram (a) is proportional to

$$\begin{aligned}&\int d^nk \frac{<4-|\gamma^\mu(\not{k}+\not{p}_4)\gamma^\alpha(1-\gamma_5)(\not{p}_1+\not{k})\gamma^\mu|1-><3-|\gamma^\alpha|2->}{k^2(k+p_4)^2(k+p_1)^2}\\ =\;& 2\int_0^1 dx\,x\int_0^1 dy\int d^nk\frac{<4-|\gamma^\mu(\not{k}+\not{p})\gamma^\alpha(1-\gamma_5)(\not{q}+\not{k})\gamma^\mu|1-><3-|\gamma^\alpha|2->}{(k^2-x^2y(1-y)s_{14})^3},\end{aligned} \tag{70}$$

where $p=-xyp_1+(1-x+xy)p_4$, and $q=(1-xy)p_1-x(1-y)p_4$. Writing γ^μ, defined in n-dimensions, as

$$\gamma^\mu = \gamma^\mu_{(4)} + \underline{\gamma}^\mu, \tag{71}$$

where $\gamma^\mu_{(4)}$ are the four dimensional Dirac matrices and

$$\begin{aligned}&\underline{\gamma}^\mu = 0 \quad \text{for} \quad \mu \le 4,\\ &[\gamma_5, \underline{\gamma}^\mu] = 0, \quad \text{for} \quad \mu > 4,\end{aligned} \tag{72}$$

the numerator in the integrand in (70) can be written as

$$\begin{aligned}&<4-|\gamma^\mu(\not{k}_{(4)}+\not{p})\gamma^\alpha_{(4)}(\not{q}+\not{k}_{(4)})\gamma^\mu_{(4)}|1-><3-|\gamma^\alpha_{(4)}|2->\\ &+<4-|\underline{\gamma}^\mu\;\not{\underline{k}}\gamma^\alpha_{(4)}\;\not{\underline{k}}\underline{\gamma}^\mu|1-><3-|\gamma^\alpha_{(4)}|2->\end{aligned} \tag{73}$$

The second term in (73) is $O(\epsilon^4)$ and so it can be safely discarded because the soft and collinear divergence is at most $O(1/\epsilon^2)$. The four-dimensional Dirac algebra then gives the divergent term

$$<4-|\gamma^\mu_{(4)}\;\not{k}_{(4)}\gamma^\alpha_{(4)}\;\not{k}_{(4)}\gamma^\mu_{(4)}|1-><3-|\gamma^\alpha_{(4)}|2-> \tag{74}$$

to

$$\frac{8k^2}{n}[12]<34>, \tag{75}$$

where k^2 is defined in n-dimensions. Then the integration over k in n dimensions can be done in the standard way [10]. For other diagrams we can similarly check that only the four dimensional γ-matrices contribute to the loop diagrams.

As mentioned before, the counter terms (g),(h) are nonvanishing only for the color octet currents. For the octet currents, from the fermion self-energy diagrams and (a),(b), they are given by

$$\frac{N_c}{2} g^2 \left(\frac{1}{\epsilon}\right) c_\Gamma \cdot \mathcal{A}_{tree}, \tag{76}$$

where $\mathcal{A}_{tree}$ denotes the tree amplitude of the corresponding contact term. Also the UV divergences in (c)-(f) should be subtracted in the $\overline{MS}$ scheme. For each helicity channel, we give $\psi^{(4,c)}_{mn}, \tilde{c}, A^{(0)}, \tilde{A}^{(1)}, B^{(0)}, \tilde{B}^{(1)}$ in appendix.

7 Drell-Yan Process

If composite quarks and leptons share common constituents, exchanges between quarks and leptons of their common constituents would give rise to quark-lepton contact interactions at low energies. Then the signal from these contact interactions may appear in Drell-Yan processes. In this section we write down a general effective quark-lepton contact interactions and consider their one-loop QCD corrections in Drell-Yan processes.

As in the EHLQ lagrangian, we consider a single family of quarks and leptons. Including more fermion families should be straightforward. With the first generation of fermions, the most general, helicity preserving, $SU(3)_{QCD} \times SU(2)_L \times U(1)_Y$ symmetric quark-lepton contact interactions are

$$\begin{aligned}
\mathcal{L}_{QL} &= \frac{g_0^2}{2\Lambda^2} \Big\{ \xi_0 \bar{q}_L \gamma^\mu \bar{q}_L \bar{l}_L \gamma^\mu l_L + \xi_1 \bar{q}_L \gamma^\mu \frac{\tau^a}{2} q_L \bar{l}_L \gamma^\mu \frac{\tau^a}{2} l_L \\
&\quad + \xi_u \bar{l}_L \gamma^\mu l_L \bar{u}_R \gamma^\mu u_R + \xi_d \bar{l}_L \gamma^\mu l_L \bar{d}_R \gamma^\mu d_R + \xi_e \bar{q}_L \gamma^\mu q_L \bar{e}_R \gamma^\mu e_R \\
&\quad + \xi_{ue} \bar{u}_R \gamma^\mu u_R \bar{e}_R \gamma^\mu e_R + \xi_{de} \bar{d}_R \gamma^\mu d_R \bar{e}_R \gamma^\mu e_R + \left(\xi_s \bar{q}^i_L d_R \bar{e}_R l^i_L + h.c. \right) \Big\},
\end{aligned} \tag{77}$$

where $l_L = (\nu, e)_L$, $q_L = (u, d)_L$. The last term in (77) is due to scalar (or pseudo scalar) exchanges and all the other terms are due to vector (or axial vector) exchanges.

For the massless fermions, no amplitudes with the same fermion helicities in the scalar exchange term arise in the standard model, and so the contact term of the scalar exchanges provides the leading amplitude in that helicity channel. Therefore we may keep the amplitudes in the scalar channel at tree-level, and consider one-loop QCD corrections only in the vector channels.

To calculate the one-loop QCD corrections in the quark sector in Drell-Yan process, we must consider virtual corrections in $q\bar{q}' \to l\bar{l}'$ and the real gluon emission in $q\bar{q}' \to l\bar{l}'G$ along with $qG \to q'l\bar{l}'$. Since these processes occur only in s-channel in the lepton momenta, the

amplitudes for a given helicity channel factorize into a flavor-independent part and a flavor-dependent propagator part that also includes the couplings on the quark and lepton vertices. The contact interactions thus modify only the propagator part, and so the one-loop QCD corrections in this model are essentially identical to those in the standard model. This allows us to write the cross section at parton level in terms of the corresponding cross section with a virtual photon exchange in the standard model

$$d\sigma^{(h)}(q\bar{q}' \to l\bar{l}') = d\sigma^{(h)}_{\gamma^*}(q\bar{q} \to l\bar{l}) \cdot \left| \frac{D^{(h)}(q\bar{q}' \to l\bar{l}')q^2}{Q_q Q_l} \right|^2 , \tag{78}$$

where $h, Q_{q,l}$ denote the helicities and charges of quarks and leptons respectively and q^2 is the invariant mass squared of the leptons. The helicity independence of $d\sigma^{(h)}_{\gamma^*}/dQ^2$, where $q^2 = Q^2$, of virtual photon exchange allows us to write (78) as

$$\frac{d\sigma^{(h)}}{dQ^2}(q\bar{q}' \to l\bar{l}') = \frac{d\sigma_{\gamma^*}}{dQ^2}(q\bar{q} \to l\bar{l}) \cdot \left| \frac{D^{(h)}(q\bar{q}' \to l\bar{l}')q^2}{Q_q Q_l} \right|^2 . \tag{79}$$

Similarly for the $qG \to q'l\bar{l}'$,

$$\frac{d\sigma^{(h)}}{dQ^2}(qG \to q'l\bar{l}') = \frac{d\sigma_{\gamma^*}}{dQ^2}(qG \to ql\bar{l}) \cdot \left| \frac{D^{(h)}(q\bar{q}' \to l\bar{l}')q^2}{Q_q Q_l} \right|^2 . \tag{80}$$

From $d\sigma_{\gamma^*}/dQ^2$ in Altarelli, Ellis and Martinelli [15], we finally have the Drell-Yan cross section for $l\bar{l}'$ pair production,

$$\begin{aligned}
\frac{d\sigma^{DY}}{dQ^2} &= \frac{1}{4}\frac{1}{36\pi s Q^2}\int_0^1 \frac{dx_1}{x_1}\int_0^1 \frac{dx_2}{x_2}\sum_{f,f'}\Big\{\Big[q_f^{[1]}(x_1)\bar{q}_{f'}^{[2]}(x_2) + (1 \leftrightarrow 2)\Big] \\
&\quad \times \Big[\delta(1-z) + \alpha_s(Q^2)\theta(1-z)(f_{q,DY}(z) - 2f_{q,2}(z))\Big] \\
&\quad + \Big[(q_f^{[1]}(x_1) + \bar{q}_{f'}^{[1]}(x_1))G^{[2]}(x_2) + (1 \leftrightarrow 2)\Big]\alpha_s(Q^2)\theta(1-z)(f_{G,DY}(z) - f_{G,2}(z))\Big\} \\
&\quad \times \sum_h \left| D^{(h)}(q_f\bar{q}_{f'} \to l\bar{l}')q^2 \right|^2 ,
\end{aligned} \tag{81}$$

with

$$\begin{aligned}
f_{q,DY} - 2f_{q,2} &= \frac{2}{3\pi}\left[\frac{3}{(1-z)_+} - 6 - 4z + 2(1+z^2)\left(\frac{\ln(1-z)}{1-z}\right)_+ + (1+\frac{4}{3}\pi^2)\delta(1-z)\right], \\
f_{G,DY} - f_{G,2} &= \frac{1}{4\pi}\left[\frac{3}{2} - 5z + \frac{9}{2}z^2 + (z^2 + (1-z)^2)\ln(1-z)\right],
\end{aligned} \tag{82}$$

where $z = Q^2/x_1x_2s$ and $\sqrt{s}$ is the invariant mass of the incoming hadron system.

From the standard model lagrangian and (77) we can read off the nonvanishing propagator part

$$
\begin{aligned}
D(u_L\bar{d}_L \to \nu_L\bar{e}_L) &= \frac{g^2}{2(q^2-M_w^2)} + \frac{g_0^2\xi_1}{4\Lambda^2},\\
D(u_L\bar{u}_L \to e_L\bar{e}_L) &= \left(\frac{g}{4\cos\theta_w}\right)^2 \frac{u_-l_-}{q^2-M_z^2} + \frac{Q_uQ_e}{q^2} + \frac{g_0^2\xi_0}{2\Lambda^2} - \frac{g_0^2\xi_1}{8\Lambda^2},\\
D(u_L\bar{u}_L \to e_R\bar{e}_R) &= \left(\frac{g}{4\cos\theta_w}\right)^2 \frac{u_-l_+}{q^2-M_z^2} + \frac{Q_uQ_e}{q^2} + \frac{g_0^2\xi_e}{2\Lambda^2},\\
D(u_R\bar{u}_R \to e_L\bar{e}_L) &= \left(\frac{g}{4\cos\theta_w}\right)^2 \frac{u_+l_-}{q^2-M_z^2} + \frac{Q_uQ_e}{q^2} + \frac{g_0^2\xi_u}{2\Lambda^2},\\
D(u_R\bar{u}_R \to e_R\bar{e}_R) &= \left(\frac{g}{4\cos\theta_w}\right)^2 \frac{u_+l_+}{q^2-M_z^2} + \frac{Q_uQ_e}{q^2} + \frac{g_0^2\xi_{ue}}{2\Lambda^2},\\
D(d_L\bar{d}_L \to e_L\bar{e}_L) &= \left(\frac{g}{4\cos\theta_w}\right)^2 \frac{d_-l_-}{q^2-M_z^2} + \frac{Q_dQ_e}{q^2} + \frac{g_0^2\xi_0}{2\Lambda^2} + \frac{g_0^2\xi_1}{8\Lambda^2},\\
D(d_L\bar{d}_L \to e_R\bar{e}_R) &= \left(\frac{g}{4\cos\theta_w}\right)^2 \frac{d_-l_+}{q^2-M_z^2} + \frac{Q_dQ_e}{q^2} + \frac{g_0^2\xi_e}{2\Lambda^2},\\
D(d_R\bar{d}_R \to e_L\bar{e}_L) &= \left(\frac{g}{4\cos\theta_w}\right)^2 \frac{d_+l_-}{q^2-M_z^2} + \frac{Q_dQ_e}{q^2} + \frac{g_0^2\xi_d}{2\Lambda^2},\\
D(d_R\bar{d}_R \to e_R\bar{e}_R) &= \left(\frac{g}{4\cos\theta_w}\right)^2 \frac{d_+l_+}{q^2-M_z^2} + \frac{Q_dQ_e}{q^2} + \frac{g_0^2\xi_{de}}{2\Lambda^2},
\end{aligned}
\tag{83}
$$

where

$$
\begin{array}{lcllcl}
u_- &=& 2-\frac{8}{3}\sin^2\theta_w; & u_+ &=& -\frac{8}{3}\sin^2\theta_w,\\
d_- &=& -2+\frac{4}{3}\sin^2\theta_w; & d_+ &=& \frac{4}{3}\sin^2\theta_w,\\
l_- &=& -2+4\sin^2\theta_w; & l_+ &=& 4\sin^2\theta_w,
\end{array}
$$

and g is the $SU(2)_L$ coupling constant.

Finally we would like to add a comment on calculating $d\sigma^{DY}/dp_l dy_l$ in the framework of Kunszt, et.al., where p_l, y_l are the transverse momentum and rapidity of a designated lepton respectively. Since the essential difference of Drell-Yan process from the one-jet inclusive production is that the soft and collinear divergences in Drell-Yan process occur only in the initial state, all the formulae for the inclusive jet cross section can be used with only minor modification. First, since the final state leptons in Drell-Yan process are identifiable, the jet algorithm in (50) should be replaced by

$$
S_2 = 2!\delta(p_l-p_1)\delta(y_l-y_1), \qquad S_3 = 3!\delta(p_l-p_1)\delta(y_l-y_1), \tag{84}
$$

and since soft and collinear divergences occur only in the initial state, the indices m, n in (57), (58), and (63) should run only over the initial state. Also the restriction on p_3 that it is the smallest among the final state parton momenta should be revoked.

For the virtual corrections, we need to consider only the diagram (a) in Fig.1, and its calculation goes exactly as in the case of the one-jet inclusive cross section. Details of the calculation and numerical analysis of the Drell-Yan cross section along with the one-jet inclusive cross section will be published elsewhere [16].

8 Acknowledgements

I am grateful to E. Eichten for interesting me in this subject and many valuable suggestions throughout the work. Also helpful discussions with and comments by S. Parke and W. Giele are gratefully acknowledged.

A Appendix

In this appendix we give the tree amplitudes $\psi^{(4,c)}_{mn}, \tilde{c}, A^{(0)}_{cont}, B^{(0)}_{cont}$, and the one-loop amplitudes $\tilde{A}^{(1)}_{cont}\tilde{B}^{(1)}_{cont}$ defined in (57), (64),(65) and (69), and for completeness, corresponding terms in QCD for the following helicity channels: (i) $u_L d_L \to u_L d_L$, (ii) $u_L u_L \to u_L u_L$, (iii) $u_R d_L \to u_R d_L$, (iv) $u_L d_R \to u_L d_R$, (v) $u_R u_R \to u_R u_R$, (vi) $d_R d_R \to d_R d_R$, and (vii) $u_R d_R \to u_R d_R$. All the momenta of external fermions are assumed to have positive energies, and $s_{ij} = (p_i + p_j)^2$.

$\tilde{\mathbf{c}}$:

	$\tilde{c}$	$\lvert\tilde{c}\rvert^2$
(i)	$-2i[12]<34>$	$4s_{12}^2$
(ii)	$-2i[12]<34>$	$4s_{12}^2$
(iii)	$-2i[24]<13>$	$4s_{13}^2$
(iv)	$-2i[13]<24>$	$4s_{13}^2$
(v)	$-2i[34]<12>$	$4s_{12}^2$
(vi)	$-2i[34]<12>$	$4s_{12}^2$
(vii)	$-2i[34]<12>$	$4s_{12}^2$

(A.1)

$\mathbf{A^{(0)}}, \mathbf{B^{(0)}}$: For contact terms,

	$A^{(0)}_{cont}$	$B^{(0)}_{cont}$
(i)	$-2\eta_0 + \eta_1/2$	$-\eta_1$
(ii)	$-2(\eta_0 + \eta_1/4)$	$-2(\eta_0 + \eta_1/4)$
(iii)	$-\eta_u + \eta_{8u}/2N_c$	$-\eta_{8u}/2$
(iv)	$-\eta_d + \eta_{8d}/2N_c$	$-\eta_{8d}/2$
(v)	$-2\eta_{uu}$	$-2\eta_{uu}$
(vi)	$-2\eta_{dd}$	$-2\eta_{dd}$
(vii)	$-\eta_{ud}$	$-\eta'_{ud}$

(A.2)

and for QCD,

	$A^{(0)}_{QCD}$	$B^{(0)}_{QCD}$
(i)	$-1/2N_c s_{14}$	$1/2s_{14}$
(ii)	$-1/2N_c s_{14} + 1/2s_{13}$	$-1/2N_c s_{13} + 1/2s_{14}$
(iii)	$-1/2N_c s_{14}$	$1/2s_{14}$
(iv)	$-1/2N_c s_{14}$	$1/2s_{14}$
(v)	$-1/2N_c s_{14} + 1/2s_{13}$	$-1/2N_c s_{13} + 1/2s_{14}$
(vi)	$-1/2N_c s_{14} + 1/2s_{13}$	$-1/2N_c s_{13} + 1/2s_{14}$
(vii)	$-1/2N_c s_{14}$	$1/2s_{14}$

$\boldsymbol{\psi^{(4,c)}_{mn}}$: For each helicity channel,

$$\begin{aligned}
\psi^{(4)} &= |\tilde{c}|^2 N_c^2 \left[\left(A^{(0)}\right)^2 + \left(B^{(0)}\right)^2 + \tfrac{2}{N_c} A^{(0)} B^{(0)}\right] \\
\psi^{(4,c)}_{12} &= \psi^{(4)}/N_c - |\tilde{c}|^2 N_c \left[\left(A^{(0)}\right)^2 + \left(B^{(0)}\right)^2 + 2N_c A^{(0)} B^{(0)}\right] \\
\psi^{(4,c)}_{13} &= -\psi^{(4)}/N_c + |\tilde{c}|^2 N_c \left[\left(A^{(0)}\right)^2 + N_c \left(B^{(0)}\right)^2\right] \\
\psi^{(4,c)}_{14} &= -\psi^{(4)}/N_c + |\tilde{c}|^2 N_c \left[N_c \left(A^{(0)}\right)^2 + \left(B^{(0)}\right)^2\right] \\
\psi^{(4,c)}_{23} &= \psi^{(4,c)}_{14},\ \psi^{(4,c)}_{24} = \psi^{(4,c)}_{13},\ \psi^{(4,c)}_{34} = \psi^{(4,c)}_{12},
\end{aligned} \tag{A.3}$$

where $A^{(0)}, B^{(0)}$ are the sum of the corresponding contact and QCD terms as defined in (66).

$\tilde{\mathbf{A}}^{(1)}, \tilde{\mathbf{B}}^{(1)}$: With the auxiliary functions,

$$\begin{aligned}
F_1 &= 2(N_c^2-1)/N_c \left[3 + \tfrac{3}{2}\ln\left(\tfrac{Q^2_{ES}}{s_{14}}\right) + \tfrac{1}{2}\ln^2\left(\tfrac{Q^2_{ES}}{s_{14}}\right)\right] \\
F_2 &= 2\left[4 + \tfrac{3}{2}\ln\left(\tfrac{Q^2_{ES}}{s_{13}}\right) + \tfrac{1}{2}\left(\ln^2\left(\tfrac{Q^2_{ES}}{s_{13}}\right) - \ln^2\left(\tfrac{Q^2_{ES}}{-s_{12}}\right)\right) + \tfrac{3}{2}\ln\left(\tfrac{\mu^2}{Q^2_{ES}}\right)\right] \\
F_3 &= -F_2(s_{12} \leftrightarrow -s_{13}),
\end{aligned} \tag{A.4}$$

and

$$\begin{aligned}
F_{1o} &= -(N_c^1-1)/N_c^2 \left[4 + \tfrac{3}{2}\ln\left(\tfrac{Q^2_{ES}}{-s_{12}}\right) + \tfrac{1}{2}\left(\ln^2\left(\tfrac{Q^2_{ES}}{-s_{12}}\right)\right.\right. \\
&\quad \left.\left. - \ln^2\left(\tfrac{Q^2_{ES}}{s_{13}}\right)\right) + \tfrac{3}{2}\ln\left(\tfrac{\mu^2}{Q^2_{ES}}\right)\right] \\
F_{2o} &= 1/N_c \left[5 - N_c^2 - \tfrac{3}{2}\ln\left(\tfrac{Q^2_{ES}}{s_{14}}\right) + 3\ln\left(\tfrac{Q^2_{ES}}{-s_{12}}\right) - \tfrac{1}{2}\ln^2\left(\tfrac{Q^2_{ES}}{s_{14}}\right)\right. \\
&\quad \left. + \ln^2\left(\tfrac{Q^2_{ES}}{-s_{12}}\right) - \left(1 - \tfrac{N_c^2}{2}\right)\left(\ln^2\left(\tfrac{Q^2_{ES}}{s_{13}}\right) - 3\ln^2\left(\tfrac{\mu^2}{Q^2_{ES}}\right)\right)\right],
\end{aligned} \tag{A.5}$$

the contact terms are

$$\begin{aligned}
&\text{(i)} && \tilde{A}^{(1)}_{cont} &&= (2\eta_0 - \eta_1/2)(F_1 - F_2/N_c) + \eta_1 F_2(p_3 \leftrightarrow p_4) \\
& && \tilde{B}^{(1)}_{cont} &&= (2\eta_0 - \eta_1/2)F_2 + \eta_1(F_1 - F_2/N_c)(p_3 \leftrightarrow p_4), \\
&\text{(ii)} && \tilde{A}^{(1)}_{cont} &&= 2(\eta_0 + \eta_1/4)\left[F_1 - F_2/N_c + F_2(p_3 \leftrightarrow p_4)\right] \\
& && \tilde{B}^{(1)}_{cont} &&= 2(\eta_0 + \eta_1/4)\left[F_2 + (F_1 - F_2/N_c)(p_3 \leftrightarrow p_4)\right], \\
&\text{(iii)} && \tilde{A}^{(1)}_{cont} &&= \eta_u(F_1 - F_3/N_c) + \eta_{8u}(F_{1o} - F_{2o}/N_c) \\
& && \tilde{B}^{(1)}_{cont} &&= \eta_u F_3 + \eta_{8u} F_{2o}, \\
&\text{(iv)} && \text{Replace} && \eta_u \to \eta_d,\ \eta_{8u} \to \eta_{8d} \text{ in (iii)}, \\
&\text{(v)} && \text{Replace} && (\eta_0 + \eta_1/4) \to \eta_{uu} \text{ in (ii)}, \\
&\text{(vi)} && \text{Replace} && (\eta_0 + \eta_1/4) \to \eta_{dd} \text{ in (ii)}, \\
&\text{(vii)} && \text{Replace} && (2\eta_0 - \eta_1/2) \to \eta_{ud},\ \eta_1 \to \eta'_{ud} \text{ in (i)}.
\end{aligned} \tag{A.6}$$

For QCD, from the one-loop amplitudes in [6], (i),(vii);

$$\begin{aligned}
\tilde{A}^{(1)}_{QCD} &= -\tfrac{1}{2 s_{14} N_c} H_1 \\
\tilde{B}^{(1)}_{QCD} &= \tfrac{1}{2 s_{14}}(H_1 + H_2),
\end{aligned} \tag{A.7}$$

(ii),(v),(vi);

$$\begin{array}{rcl}\tilde{A}^{(1)}_{QCD} &=& \frac{1}{s_{14}}\left[-H_1/N_c + \frac{s_{14}}{s_{13}}\left[(H_1+H_2)\,(p_3 \leftrightarrow p_4)\right]\right] \\ \tilde{B}^{(1)}_{QCD} &=& \frac{1}{s_{14}}\left[H_1 + H_2 - \frac{s_{14}}{N s_{13}} H_1(p_3 \leftrightarrow p_4)\right],\end{array} \tag{A.8}$$

(iii),(iv);

$$\begin{array}{rcl}\tilde{A}^{(1)}_{QCD} &=& -\frac{1}{2 s_{14} N_c} K_1 \\ \tilde{B}^{(1)}_{QCD} &=& \frac{1}{2 s_{14}}(K_1 + K_2),\end{array} \tag{A.9}$$

where

$$\begin{array}{rcl}
H_1 &=& N_c(13/9+\pi^2) - \frac{10}{9}N_f + \frac{1}{N_c}\left[8 + \frac{s_{14}}{2s_{12}}(1+s_{13}/s_{12})\left(\ln^2\left(\frac{-s_{14}}{s_{12}}\right)+\pi^2\right)\right. \\
&& \left. + s_{14}/s_{12}\ln\left(\frac{s_{14}}{s_{13}}\right)\right] + \ln\left(\frac{Q^2_{ES}}{s_{14}}\right)\left[-3N_c + \frac{11}{3}N_c - 2\ln\left(\frac{-s_{14}}{s_{12}}\right) - \frac{2}{3}N_f\right. \\
&& \left. + 3/N_c + 2/N_c \ln\left(\frac{s_{12}}{-s_{13}}\right)\right] - \ln^2\left(\frac{Q^2_{ES}}{s_{14}}\right)(N_c - 1/N_c) + 4\pi\beta_0 \ln\left(\frac{\mu^2}{Q^2_{ES}}\right), \\
H_2 &=& -(N_c^2-1)/N_c\left[\frac{1}{2}\frac{s_{14}}{s_{12}}(1+s_{13}/s_{12})\left(\ln^2\left(\frac{s_{14}}{s_{13}}\right)+\pi^2\right)\right. \\
&& \left. + s_{14}/s_{12}\ln\left(\frac{s_{14}}{s_{13}}\right) + 2\ln\left(\frac{Q^2_{ES}}{s_{14}}\right)\ln\left(\frac{s_{12}}{-s_{13}}\right)\right], \\
K_1 &=& N_c(13/9+\pi^2) - \frac{10}{9}N_f + 8/N_c + (N_c + 1/N_c)\left[\frac{s_{14}}{2s_{13}}(1+s_{12}/s_{13})\right. \\
&& \left.\left(\ln^2\left(\frac{s_{14}}{s_{13}}\right)+\pi^2\right) + s_{14}/s_{13}\ln\left(\frac{-s_{14}}{s_{12}}\right)\right] + \ln\left(\frac{Q^2_{ES}}{s_{14}}\right)\left[-3N_c + \frac{11}{3}N_c\right. \\
&& \left. - 2N_c\ln\left(\frac{-s_{14}}{s_{12}}\right) - \frac{2}{3}N_f + 3/N_c + 2/N_c\ln\left(\frac{s_{12}}{-s_{13}}\right)\right] \\
&& + \ln^2\left(\frac{Q^2_{ES}}{s_{14}}\right)(-N_c + 1/N_c) + 4\pi\beta_0\ln\left(\frac{\mu^2}{Q^2_{ES}}\right), \\
K_2 &=& -(N_c^2-1)/N_c\left[\frac{s_{14}}{2s_{13}}(1+s_{12}/s_{13})\left(\ln^2\left(\frac{-s_{14}}{s_{12}}\right)+\pi^2\right)\right. \\
&& \left. + s_{14}/s_{13}\ln\left(\frac{-s_{14}}{s_{12}}\right) + 2\ln\left(\frac{Q^2_{ES}}{s_{14}}\right)\ln\left(\frac{s_{12}}{-s_{13}}\right)\right].
\end{array} \tag{A.10}$$

References

[1] Inclusive Jet Cross Section in $\bar{p}p$ collisions at $\sqrt{2} = 1.8$ TeV, F. Abe, et.al., FERMILAB-PUB-96/020-E.

[2] E. Eichten, K.Lane, and M.Peskin, Phys. Rev. Lett. 14, 811 (1983).

[3] E. Eichten, I. Hinchliffe, K. Lane, and C. Quigg, Rev. Mod. Phys. 56, 579 (1984).

[4] R.K. Ellis and J. Sexton, Nucl. Phys. B 269 (1986) 445.

[5] Z. Bern and D. Kosower, Nucl. Phys. B 379 (1992) 451.

[6] Z. Kunszt, A. Signer and Z. Trocsanyi, Nucl. Phys. B 411 (1994) 397.

[7] Z. Kunszt and D. Soper, Phys. Rev. D 46, 192 (1992).

[8] M. Mangano and S. Parke, Phys. Rep. 200 (1991) 301.

[9] M. Chanowitz and S. Drell, Phys. Rev. Lett. 30, 807 (1973).

[10] G. Guberina, R. Peccei, and R. Rueckl, Nucl. Phys. B 171 (1980) 333.

[11] K. Wilson, Phys. Rev. 179, 1499 (1969).

[12] F. Gilman and M. Wise, Phys. Rev. D 20, 2392 (1979).

[13] G. Altarelli, G. Curci, G. Martinelli, and S. Petrarca, Nucl. Phys. B 187 (1981) 461.

[14] 't Hooft and M. Veltman, Nucl. Phys. B 44 (1972) 189.

[15] G. Altarelli, R.K. Ellis, and G. Martinelli, Nucl. Phys. B 157 (1979) 461.

[16] W. Kilgore and T. Lee, in preparation.

Figure Captions:

Fig. 1: One-loop diagrams from contact interactions. (g), (h) are the counterterms for the octet current renormalization.
Fig. 2: One-loop diagram from dimension six operator. (b) is suppressed by a factor s/Λ^2 compared to the diagrams in Fig. 1.
Fig. 3: Penguin diagrams induce form factors in quark-gluon vertex.



(a) (b) (c) (d)



(e) (f) (g) (h)

Fig.1



(a) (b)

Fig.2

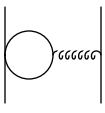


Fig.3